

**Table S.1** Target polyphenols. CAS number, molecular mass and retention time.

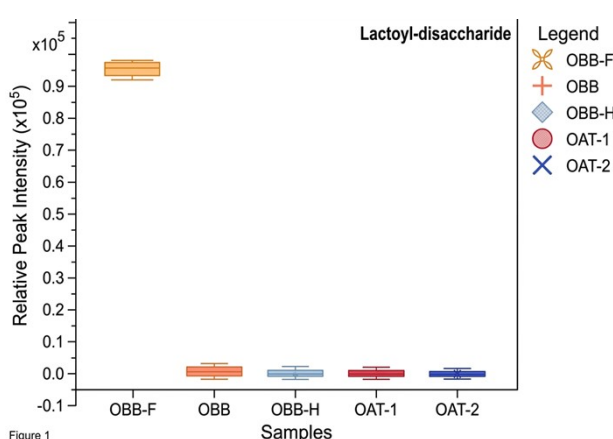
Polyphenols	CAS	Molecular mass (g·mol <sup>-1</sup> )	Retention time (min)	Precursor ion (m/z)
Gallic acid	149-91-7	170.1	2.35	169.0
2,4,6-trihydroxybenzoic acid	71989-93-0	188.1	3.37	168.9
Gallocatechin	970-73-0	306.3	3.80	305.0
3,4-dihydroxybenzoic acid	99-50-3	154.1	3.88	152.9
2,4-dihydroxybenzoic acid	89-86-1	154.1	4.41	153.0
2,5-dihydroxybenzoic acid	490-79-9	154.1	4.44	153.0
Caftaric acid	67879-58-7	312.2	4.48	310.9
2,5-dihydroxybenzaldehyde	1194-98-5	138.1	4.63	136.9
3,4-dihydroxybenzaldehyde	139-85-5	138.1	4.64	136.9
3-hydroxybenzoic acid	99-06-9	138.1	5.15	137.0
4-hydroxybenzoic acid	99-96-7	138.1	5.18	137.0
Procyanidin B1	20315-25-7	578.5	5.30	577.0
Catechin	18829-70-4	290.3	5.34	289.0
2,6-dihydroxybenzoic acid	303-07-1	154.1	5.54	153.0
3,5-dihydroxybenzoic acid	99-10-5	154.1	5.54	153.0
3-hydroxybenzaldehyde	100-83-4	122.1	5.67	121.0
4-hydroxybenzaldehyde	123-08-0	122.1	5.67	121.0
3,4-dimethoxybenzoic acid	93-07-2	182.0	6.03	182.9
Procyanidin B2	29106-49-8	578.5	6.10	577.0
Chlorogenic acid	327-97-9	354.3	6.12	353.0
Ampelopsin	27200-12-0	320.25	6.20	319.0
Caffeic acid	331-39-5	180.2	6.50	178.8
Procyanidin C1	37064-30-5	866.8	6.52	577.0
Epicatechin	35323-91-2	290.3	6.56	289.0
Epigallocatechin gallate	989-51-5	458.4	6.79	457.1
Procyanidin A1	12798-56-0	576.5	6.80	577.0
Gallocatechin gallate	84650-60-2	458.4	7.29	457.1
Procyanidin A2	41743-41-3	576.5	7.32	577.0
Orientine	28608-75-5	448.4	7.38	477.1
7-hydroxycoumarin	93-35-6	162.1	7.80	162.9
4-hydroxycinnamic acid	501-98-4	164.2	7.89	163.0
Epicatechin gallate	1257-08-5	442.4	7.92	441.1
Polidatin	27208-80-6	390.4	7.98	389.1
Taxifolin	480-18-2	304.25	8.06	303.0
Catechin gallate	130405-40-2	442.3	8.12	441.1
3,4-dimethoxybenzaldehyde	120-14-9	166.2	8.33	167.0
Trans-ferulic acid	537-98-4	194.2	8.92	192.8
4-methoxybenzaldehyde	123-11-5	136.1	9.11	136.9
Resveratrol	501-36-0	228.07	9.31	227.1
Robinetin	490-31-3	302.23	9.50	301.2
Quercetin-3-glucuronide	22688-79-5	478.4	9.54	479.0
Quercetin-3-rutinoside	153-18-4	610.5	9.72	609.1
Quercetin-3-glucoside	482-35-9	463.4	9.75	465.0
Myricetin	529-44-2	318.2	10.09	319.0
Ellagic acid	476-66-4	302.19	10.21	301.0
Rosmarinic acid	20283-92-5	360.3	10.37	359.0
3,4,5-trimethoxycinnamic acid	90-50-6	238.2	11.13	239.0
Astragalin	480-10-4	448.4	11.16	447.0
3,5-dimethoxybenzaldehyde	7311-34-4	166.2	11.26	167.1
Fisetin	528-48-3	286.2	11.50	285.0
Daidzein	486-66-8	254.2	11.53	253.0
Epsilon-viniferin	62218-08-0	454.5	11.82	455.1
Quercetin	117-39-5	302.2	11.83	303.0
Naringenin	67604-48-2	272.2	11.89	272.0
Luteolin	491-70-3	286.2	12.17	285.0
Kaempferol	520-18-3	286.2	12.35	285.0
Isorhamnetin	480-19-3	316.3	12.52	317.0
Diosmetin	520-34-3	300.26	12.64	299.0
Apigenin	520-36-5	270.2	12.63	269.0
Chrysin	480-40-0	254.2	13.24	253.1

## Supplementary Section S1. Metabolomic Identification: Beyond Tentative Approaches

After isolating the marker analytes for each group, we proceed to identify them using an initial metabolomic approach. Using analytical databases and spectral libraries, provisional names are assigned to 107 compounds, which will be refined later to achieve a complete characterization. This screening is performed using a rigorous computational algorithm that considers the analyte's location in the time-mass-intensity plane, the exact mass ( $\Delta m/z$ ), and the deviation of the isotopic pattern from its theoretical value, quantified as mSigma by the T-Rex 3D algorithm (MetaboScape®). The maximum acceptable  $\Delta m/z$  values are set at 5 mDa for the compound's mass and 50 mSigma for the isotopic pattern.

To increase the reliability of the characterization, the algorithm's scope is expanded by integrating additional tools that enable compound search, *in silico* fragmentation, and spectral comparison via MS/MS matches. The combination of these strategies provides a comprehensive and reliable identification of the analytes present.

As an example, the identification process for the analyte with  $m/z$  773, detected exclusively in the beverage fermented by *Lactobacillus plantarum*, is shown (Supplementary section S1.1).



**Supplementary section S1.1.** Relative response of the compound identified as lactoyl-disaccharide in the different samples of base oat beverage (OBB), heat-treated oat beverage (OBB-H), and *L. plantarum*-mediated fermented oat beverage (OBB-F), as well as the oat varieties used, OAT-1 and OAT-2.

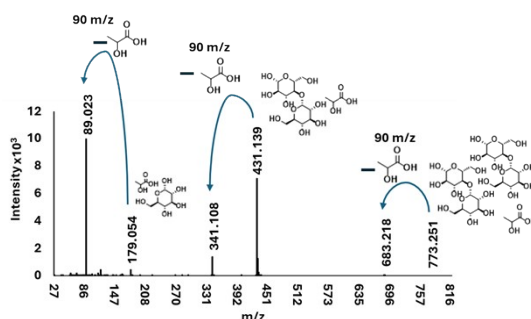
The provisional molecular formula proposed by SmartFormula is C<sub>34</sub>H<sub>46</sub>O<sub>20</sub>, based on the screening parameters mSigma < 50 and  $\Delta m/z$  < 5 mDa (Supplementary section S1.2)

Generate <input checked="" type="checkbox"/> Auto <input style="border: none; padding: 2px 5px;" type="button" value="→ Open in SF3D"/> <input style="border: none; padding: 2px 5px;" type="button" value="⚙️"/>								
IDENTIFIED COMPOUNDS								
#	Neutral Formula	Ion Formula	Ion	M calc.	m/z calc.	m/z meas.	$ \Delta m/z $ [ppm]	mSigma
1	C <sub>34</sub> H <sub>46</sub> O <sub>20</sub>	C <sub>34</sub> H <sub>45</sub> O <sub>20</sub> <sup>-</sup>	[M-H] <sup>-</sup>	774.2582	773.25096742	773.2506	0.3643	28.90
2	C <sub>52</sub> H <sub>38</sub> O <sub>7</sub>	C <sub>52</sub> H <sub>37</sub> O <sub>7</sub> <sup>-</sup>	[M-H] <sup>-</sup>	774.2618	773.25447711	773.2506	3.8740	173.35
3	C <sub>59</sub> H <sub>34</sub> O <sub>2</sub>	C <sub>59</sub> H <sub>33</sub> O <sub>2</sub> <sup>-</sup>	[M-H] <sup>-</sup>	774.2559	773.24860388	773.2506	1.9992	219.51

**Supplementary section S1.2.** List of candidates obtained using SmartFormula based on exact mass  $\Delta m/z$  and mSigma.

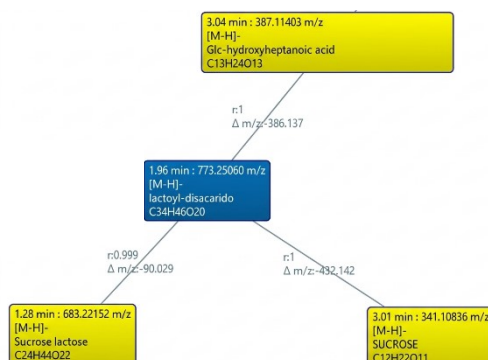
The identification is supplemented by various spectral databases integrated into MetaboScape®, which suggest possible disaccharide linkages with lactoylated bonds. The potential compound, termed lactoyl-disaccharide, exhibits the characteristic ions  $m/z$  773, 683, 431, 341, 179, and 89. This mass profile matches various carbohydrates and disaccharides, such as isomaltulose (MSBNK-RIKEN\_ReSpect-PS020108) and lactic acid units (MSBNK-Metabolon-MT000003), according to the MassBank database (<https://massbank.eu/MassBank/>).

The structural proposal is validated by *in silico* fragmentation, identifying the characteristic ions of highest intensity. The  $m/z$  773  $\rightarrow$  683 transition corresponds to a neutral loss of 90 Da, attributed to the elimination of a lactic acid residue (C<sub>3</sub>H<sub>6</sub>O<sub>3</sub>). The  $m/z$  683  $\rightarrow$  341 transition suggests the breakdown of the polysaccharide backbone into simpler subunits, while the  $m/z$  431  $\rightarrow$  341 transition could be attributed to a second loss of lactic acid, reinforcing the identification of the lactoyl-disaccharide (**Supplementary section S1.3**).



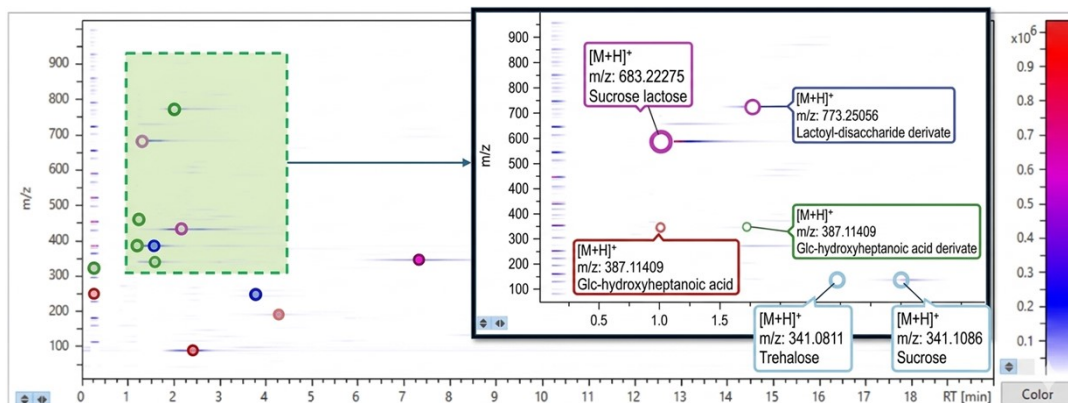
**Supplementary section S1.3.** Mass spectrum and characteristic fragmentation of the lactoyl-disaccharide analyzed using MetFrag.

All analytes identified in the several samples are grouped into a single container called a 'Bucket' in MetaboScape®, enabling the comparison of mass spectra across all samples. Comparison using MS/MS Bucket Matches reveals a high correlation ( $r > 0.9$ ) between the analyte under study and various carbohydrates, including sucrose, lactosylated derivatives and hydroxylated conjugates (**Supplementary section S2.4**).



**Supplementary section S1.4.** Spectral correlation using MS/MS bucket matches for the  $m/z$  773 ion, provisionally identified as lactoyl-disaccharide.

The topographic map illustrates the intensity of the compounds using dot size, as well as retention times and mass-to-charge ratios ( $m/z$ ). A specific region containing carbohydrates such as sucrose, trehalose, and lactoylated and hydroxylated derivatives can be observed, which supports the proposed identification of lactoyl-disaccharide (Supplementary section S1.5).

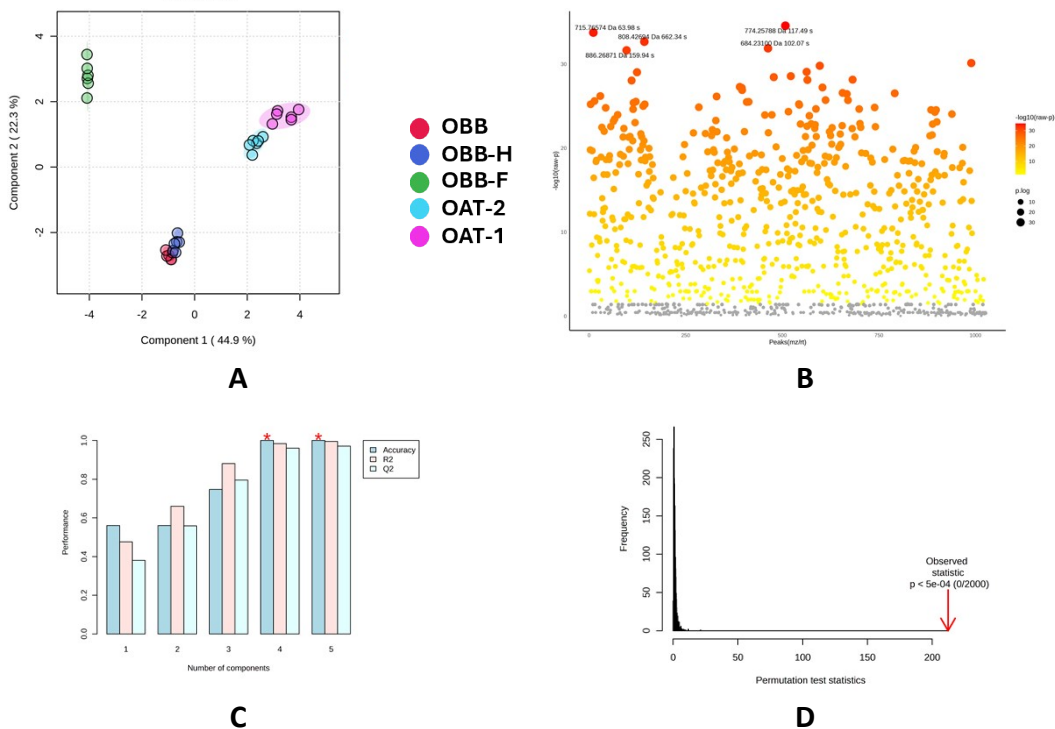


**Supplementary section S1.5.** Topographic map of the  $m/z$  773 ion and comparison with other carbohydrates present in the sample.

The combination of identification tools allows the analytes to be robustly narrowed down to a basic structure. However, the existence of possible isomers and variations in glycosylation contributes to the complexity of achieving an unambiguous identification. For this reason, the designation 'lactoyl-disaccharide' is assigned as a general name when the structure is consistent with more than one molecular distribution, and the designation 'derivative' is used when the identification only allows the analyte to be classified as part of a family of compounds or as a derivative of a specific compound.

## Supplementary section S2. Statistical study parameters via Metaboanalyst 6.0

All data were filtered using the relative standard deviation  $RSD > 25\%$  and normalised by summation. The separation of the data corresponding to the oat-based, heat-treated and fermented beverages, was carried out using both principal component analysis (PCA) and Partial Least Squares - Discriminant Analysis (PLS-DA). For the selection of representative compounds in each group, a one-way ANOVA with false discovery rate (FDR)  $p < 0.05$  was performed. By means of the 5-component evaluation, the values of PC1 and PC2 that provided adequate discrimination and representation of the data were established. The predictive capacity of the model Q2 and the determination coefficient  $R^2$  were determined as model evaluation parameters (**Supplementary section S2.1**).



**Supplementary section S2.1.** Metabolomics analysis of the different samples of base oat beverage (OBB), heat-treated oat beverage (OBB-H), and *L. plantarum*-mediated fermented oat beverage (OBB-F), as well as the oat varieties used, OAT-1 and OAT-2. Partial least squares discriminant analysis (PLS-DA) (**S2.1.A**), one-way ANOVA (**S2.1.B**), optimal number of components for PLS-DA classification by cross-validation (**S2.1.C**) and permutation of 2000 iterations (**S2.1.D**).

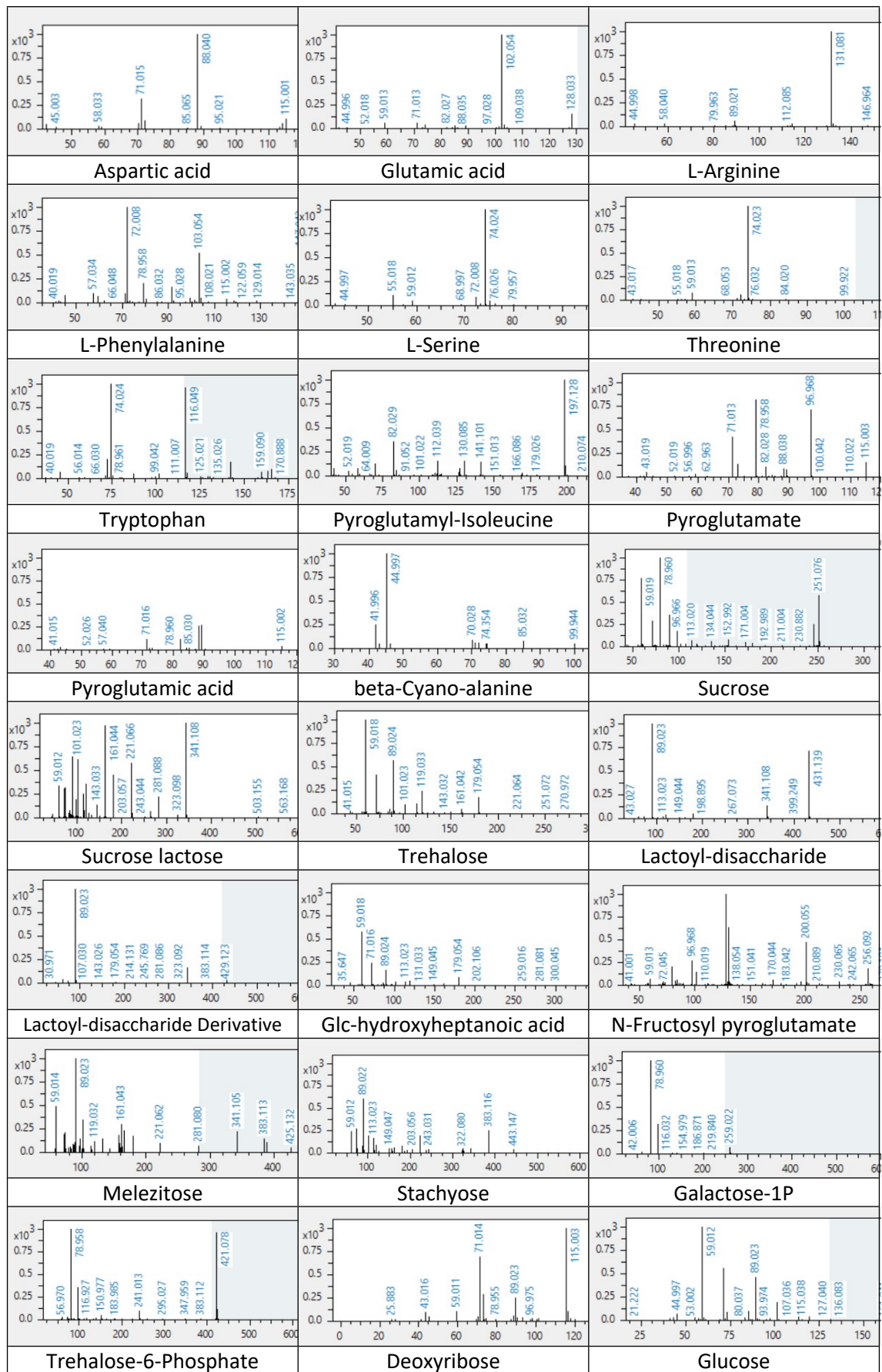


**Figure S1.** Overview of mass spectra from untargeted metabolomic analysis (Continued 1).

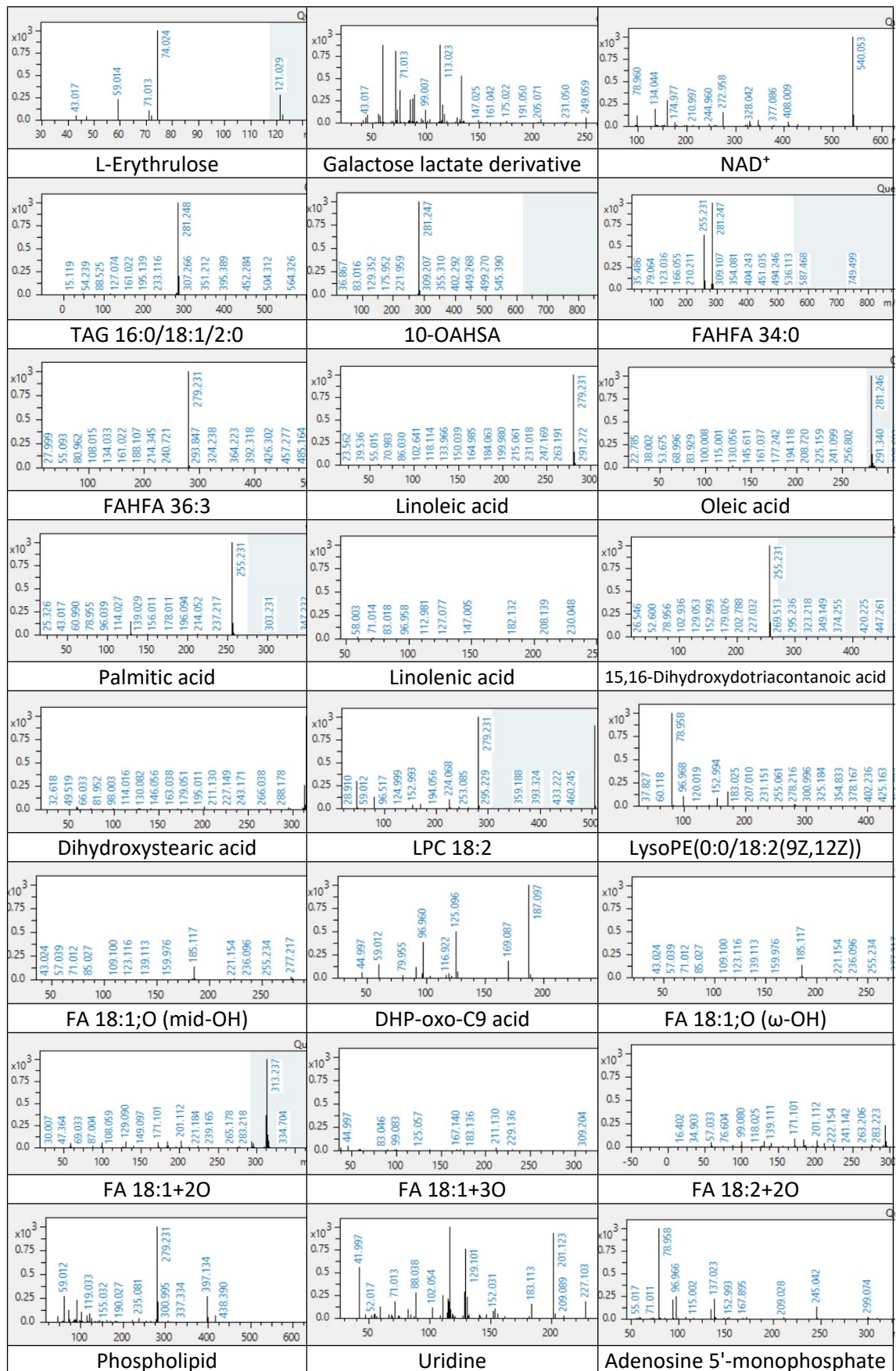


**Figure S1.** Overview of mass spectra from untargeted metabolomic analysis (Continued 2).

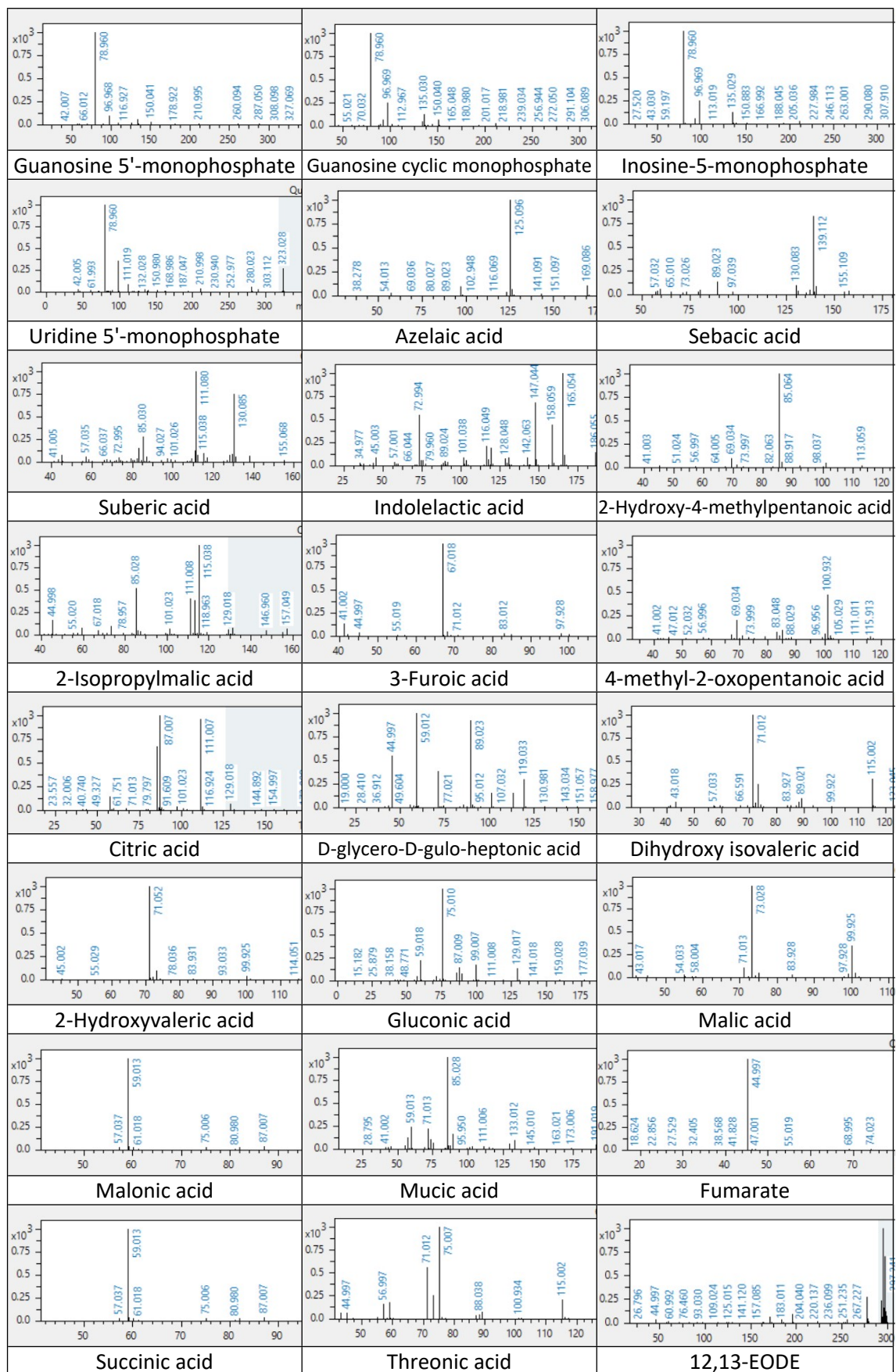


**Figure S1.** Overview of mass spectra from untargeted metabolomic analysis (Continued 3).

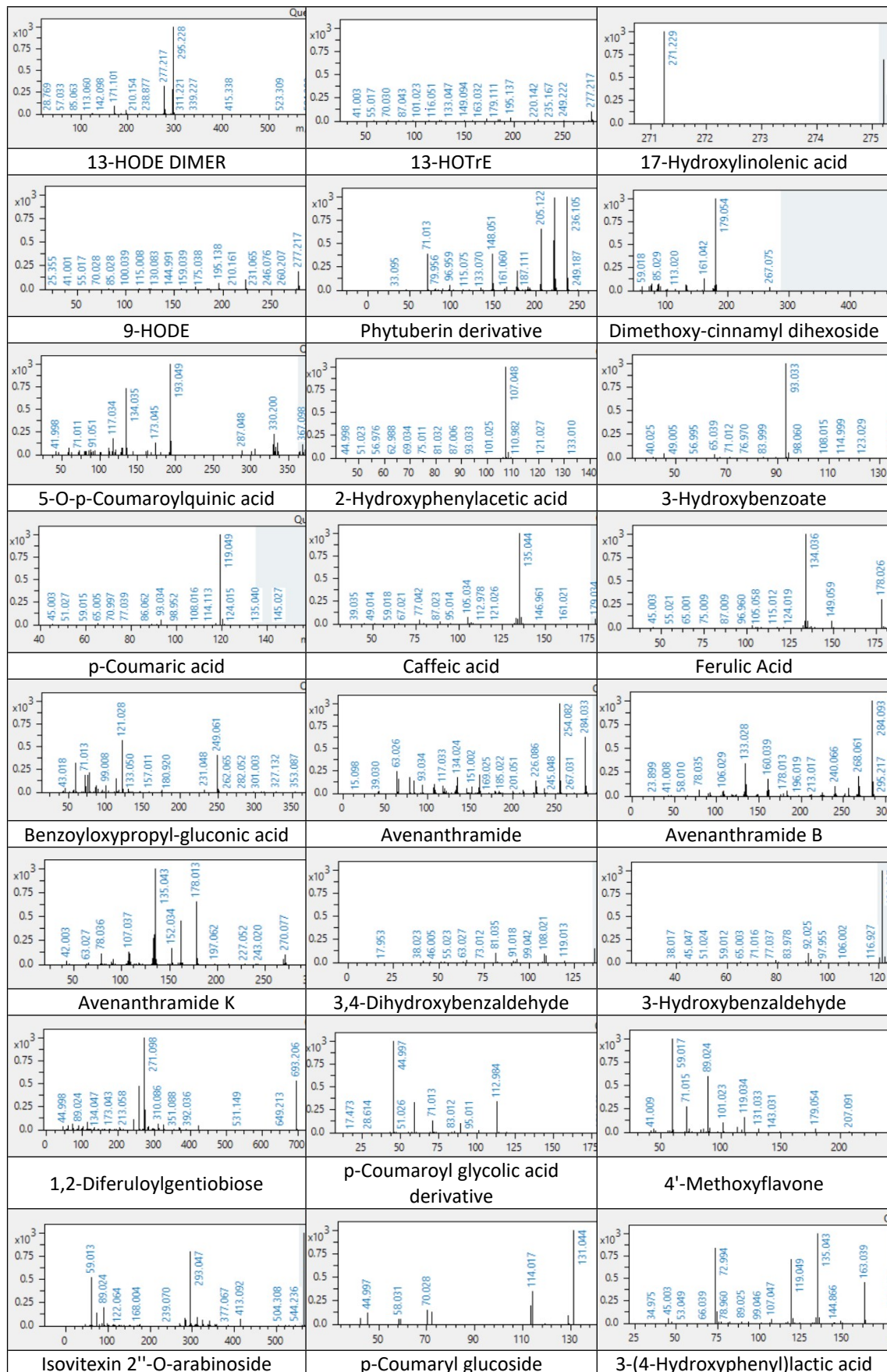
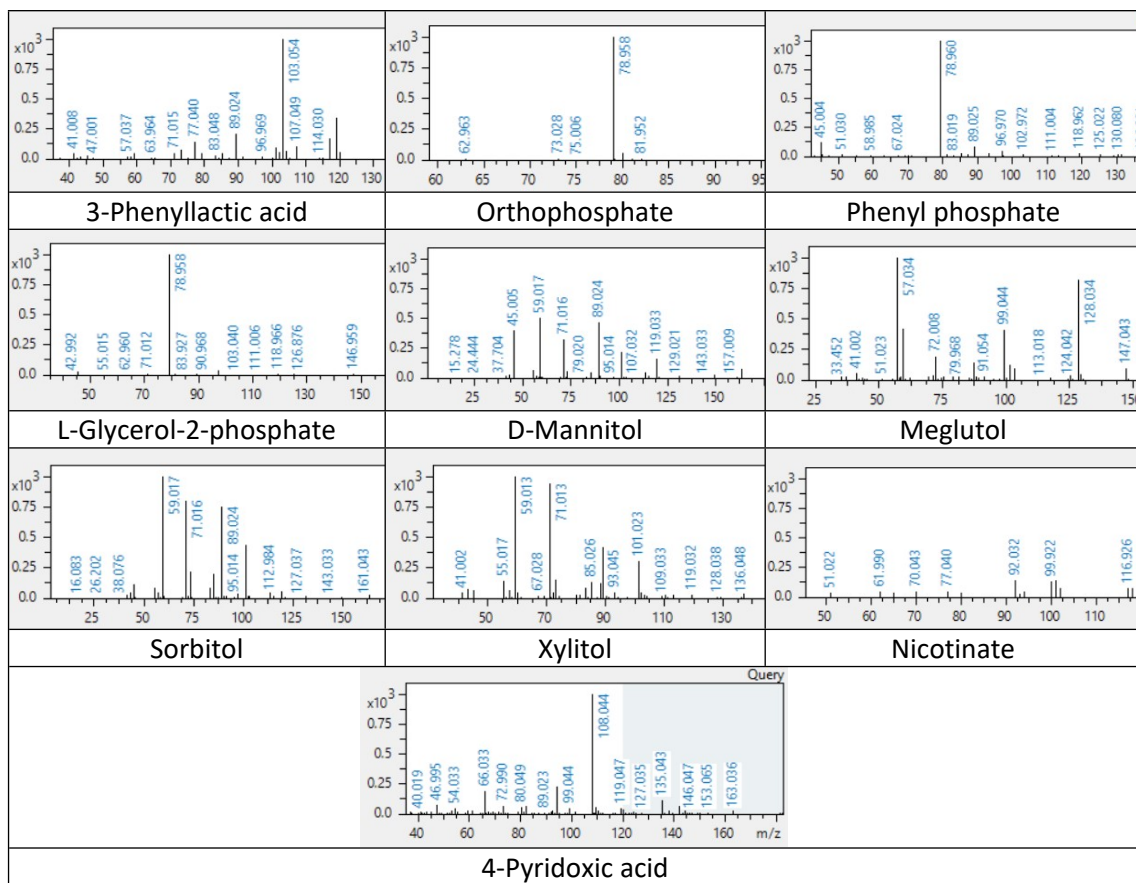


Figure S1. Overview of mass spectra from untargeted metabolomic analysis (Continued 4).



**Figure S1.** Overview of mass spectra from untargeted metabolomic analysis (Continued 5).